Barium Hydroxide as an Interlayer Between Zinc Oxide and a Luminescent Conjugated Polymer for Light-Emitting Diodes

Li Ping Lu, Dinesh Kabra, and Richard H. Friend**

A study of hybrid light-emitting diodes (HyLEDs) fabricated with and without solution-processible Cs_2CO_3 and $Ba(OH)_2$ inorganic interlayers is presented. The interlayers are deposited between a zinc oxide electron-injection layer and a fluorescent emissive polymer poly(9-dioctyl fluorine–alt-benzothiadiazole) (F8BT) layer, with a thermally evaporated MoO_3/Au layer used as top anode contact. In comparison to Cs_2CO_3, the $Ba(OH)_2$ interlayer shows improved charge carrier balance in bipolar devices and reduced exciton quenching in photoluminance studies at the ZnO/$Ba(OH)_2$/F8BT interface compared to the Cs_2CO_3 interlayer. A luminance efficiency of ≈28 cd A^{-1} (external quantum efficiency (EQE) ≈ 9%) is achieved for ≈1.2 μm thick single F8BT layer based HyLEDs. Enhanced out-coupling with the aid of a hemispherical lens allows further efficiency improvement by a factor of 1.7, increasing the luminance efficiency to ≈47cd A^{-1}, corresponding to an EQE of 15%. The photovoltaic response of these structures is also studied to gain an insight into the effects of interfacial properties on the photoinduced charge generation and back-recombination, which reveal that $Ba(OH)_2$ acts as better hole blocking layer than the Cs_2CO_3 interlayer.

1. Introduction

Since the discovery of electroluminescence from polymer based light-emitting diodes (PLEDs),[1] many efforts have been made to explore potential applications such as display panels, solid state lighting and laser diodes, due to the advantages of flexibility, ease of fabrication and large area processing. However, high production costs due to expensive deposition techniques and the use of reactive materials still limit the market entry of PLEDs and the demand for novel concepts. The on-going research in this field led to hybrid architectures integrating inorganic and organic materials, which offers an avenue to air-stable electrode geometry, with advantages of further improved device performance and stability.[2–7] The inorganic materials used have included n-type and p-type transition-metal oxides, which possess excellent transparency, good electrical conductivity, tuneable morphology and the possibility of low-cost deposition over large areas, making them ideal for PLED applications.[8,9] The study of p-type metal oxides has revealed that MoO_3 forms an ohmic contact for hole injection, as it is characterised by a low-lying lowest unoccupied molecular orbital (LUMO) level, at 6.9 eV, which is lower than the HOMO of most π-conjugated polymers. This makes MoO_3 the most promising p-type metal-oxide for the inverted PLED structure until now.[10] We and others have found that ZnO via spray pyrolysis shows very promising properties as an electron injection interlayer.[3,6,7,11] Various efforts have been made to improve electron injection by modifying the ZnO surfaces with a thin inorganic or organic interlayer.[9,12,13] Our previous studies reveal that the coating of the Cs_2CO_3 interlayer onto ZnO gives high device efficiency, as it acts as hole-blocking layer,[14] but may also dopes F8BT polymer (see chemical structure in **Figure 1**a) at interface through Cs ion diffusion.[15] However, we note that divalent earth metals, such as calcium or barium, have been used as the protecting metal to prevent defects formation on deposition of Al metal on conjugated polymers.[16] The highest efficiency for the F8BT based PLED until now have been reported using an inorganic interlayer, Cs_2CO_3.[7]

Here, we report that holes injection and transport is better than that for electrons. We focus our studies here on solution processible inorganic interlayers of barium salts, $Ba(OH)_2$ and barium acetylacetonate ($Ba(acac)_2$) in order to investigate the effect on carrier balance and device performance in inverted structure, and by comparing the results with those widely reported using Cs_2CO_3 as an electron injection layer and hole blocking layer.[6,7,11,14] We also carried out steady-state and transient photovoltaic measurements on these PLED structures to further understand the role of these inorganic interfacial modifiers and transport mechanism for injected charge carriers. This technique is similar to that used in recent reports by Blom et al. on the role of trap-assisted recombination in poly(phenylene-vinylene) (PPV) based PLEDs.[17,18] Our studies reveal the extent of photoinduced charge generation at the interface, both with and without the hole-blocking interlayer, and the role of these interlayers on the back recombination of photogenerated charge carriers. Our photovoltaic studies are hence consistent with results obtained for HyLEDs, in terms of understanding the influence of different interlayers on device performance.

L. P. Lu, Dr. D. Kabra, Prof. R. H. Friend
Cavendish Laboratory
JJ Thomson Avenue, Cambridge, CB3 0HE, UK
E-mail: dk366@cam.ac.uk; rhf10@cam.ac.uk

DOI: 10.1002/adfm.201200850

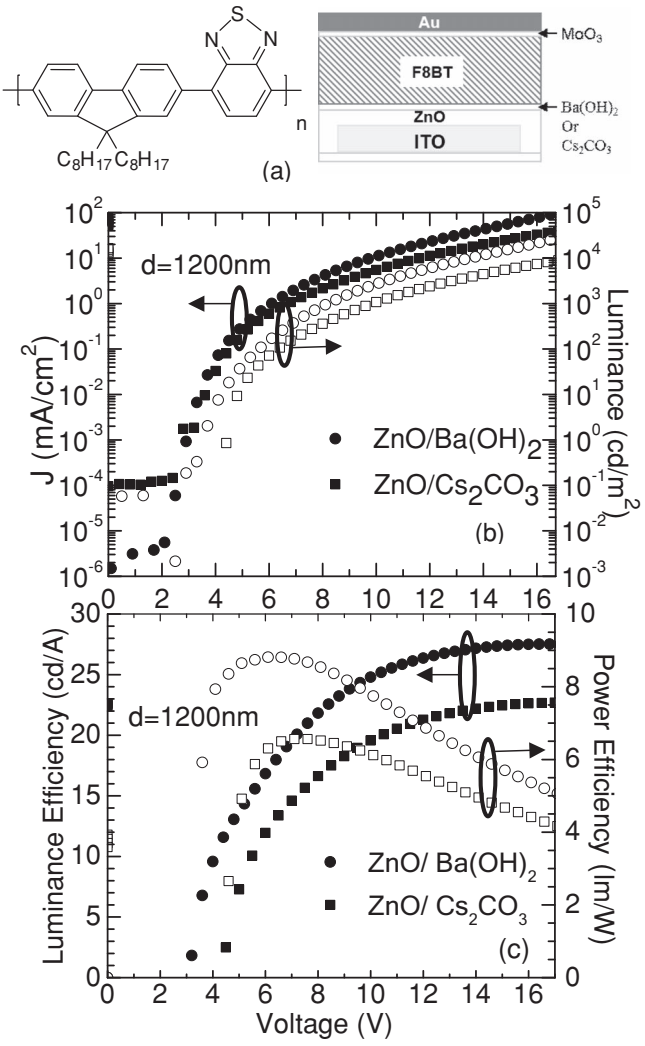

Figure 1. a) Chemical structure of F8BT polymer and Device Structure ITO/ZnO/interlayer/F8BT/MoO_3/Au of HyLED. b) J–V–L characteristics and c) derived luminance (solid) and power (open) efficiency of HyLEDs with a F8BT film thickness of 1200 nm.

2. Results

2.1. Optical Studies

We studied the role of interlayers on the optical properties of F8BT, by means of photoluminescence (PL) spectroscopy and fluorescence lifetime measurements. We spin-coated thin polymer films in order to see the influence of different interlayers on the PL quantum yield (PLQY) (thickness ≈ 30 nm) and fluorescence decay time (thickness ≈ 15 nm) of the F8BT polymer film, as shown in **Table 1** (also see in Figure S1b, Supporting Information). We find that the time evolution is well described by a mono-exponential decay rate (shown in Table 1). We note therefore that these films must be sufficiently thin that all photogenerated excitons are in communication with the

Table 1. PL quantum efficiencies (η_{PL}) and fluorescence decay times for different architectures.

Sample	η_{PL} [%]	Decay Time [ns]
F8BT	71	1.84
ZnO/Cs_2CO_3/F8BT	37	1.13
ZnO/$Ba(OH)_2$/F8BT	46	1.22

modified ZnO substrates, consistent with literature reports for the exciton diffusion range.[19] We did not observe any obvious change in the PL spectra of F8BT films with and without inorganic interlayers prepared on quartz substrates, so we exclude any possibility of the F8BT chains orientation being different on than on the bare ZnO substrates by study of PL spectrums (see Supporting Information Figure S1a). These results suggest that both interlayers cause quenching of photoluminescence at the interface; however, this quenching is greater for the Cs_2CO_3 interlayer, as compared to $Ba(OH)_2$. Both of these optical studies are consistent within experimental error (±5%) of PL quantum yield measurements, as shown by following Equation 1:

$$\frac{1}{\tau} = \frac{1}{\tau_r} + \frac{1}{\tau_{nr}}; \quad \eta_{PL} = \frac{1/\tau_r}{1/\tau_r + 1/\tau_{nr}} \Rightarrow \tau = \tau_r \eta_{PL} \qquad (1)$$

where, τ is measured fluorescence decay time, τ_r is radiative lifetime, τ_{nr} is non-radiative lifetime and η_{PL} is PL quantum yield. The low PL quantum yield for Cs_2CO_3 based sample may be due to diffusion of decomposed Cs_2CO_3 (on thermal annealing) and the interaction of Cs^{1+} ion with the BT unit of the polymer that create sub-band gap states, which possibly quench photoluminescence, as suggested by previous photoelectron spectroscopy studies.[15,20] We cannot exclude the possible role of interfacial diffusion of ionic species of barium and cesium in F8BT film at this length scale, i.e., ≈15 nm. Nevertheless, these optical studies revealed that we were able to reduce exciton quenching by using $Ba(OH)_2$ interlayer as compared to Cs_2CO_3 interlayer.

2.2. Bipolar and Single Carrier Devices

HyLEDs were fabricated with $Ba(OH)_2$ and Cs_2CO_3 interlayers and the device structure is shown in Figure 1a. The emissive polymer layer thickness was kept at 1200 nm, which was found to be optimum in our F8BT thickness dependence studies.[7] Figure 1b shows the current density with respect to operating voltage for $Ba(OH)_2$ and Cs_2CO_3 based HyLEDs. We found there is a threshold for current onset at operating bias of ≈2 V and above this threshold bias current increase rapidly. We found current density and luminance was higher for $Ba(OH)_2$ as compare to Cs_2CO_3 based HyLEDs for operating voltages above threshold (knee) voltage, i.e., above ≈2 V. These results are summarized in **Table 2**. Below the threshold a higher current density was observed in the case of Cs_2CO_3 based diode

Table 2. Comparison of HyLEDs characteristic parameters between $Ba(OH)_2$ and Cs_2CO_3 interlayer based devices and corrected parameters using an out-coupling hemisphere with a diameter of 8 mm.

Hybrid Structure F8BT [1200 nm]	$Ba(OH)_2$	Cs_2CO_3	$Ba(OH)_2$ [using hemisphere]
Bias at 10 mA/cm^2	9.9 V	11.7 V	9.9 V
Bias at 1000 cd/m^2	8.3 V	9.9 V	7.5 V
Peak luminance efficiency [cd/A]	27.6 at 17.2 V	22.7 at 16.4 V	46.8 at 16 V
Peak EQE [%]	8.9	7.3	15.1
Power efficiency at 1000cd/m^2 [lm/W]	≈9	≈6	15

(see Figure 1b). We also used $Ba(acac)_2$ as another barium based interlayer and found that operating voltages were significantly lower (5.5 V at 1000 cd/m^2) as compared to $Ba(OH)_2$ (8.3 V at 1000 cd/m^2) with similar threshold voltage ≈2 V, the corresponding efficiency was, however, up to ≈21 cd/A compared to 28 cd/A for $Ba(OH)_2$ (see Supporting Information Figure S2), It is difficult to handle $Ba(acac)_2$ due to its extremely hygroscopic nature, and the device yield was low, so that we used $Ba(OH)_2$ in the remainder of the studies reported here. Electroluminescence (EL) studies for the ITO/ZnO/interlayer/F8BT/MoO_3/Au structure showed no significant change in EL spectra (measured at J = 0.5 mA/cm^2), when comparing the $Ba(OH)_2$ and Cs_2CO_3 interlayers based HyLEDs (see Supporting Information Figure S1a). Luminance and power efficiency derived from Figure 1b are shown in Figure 1c, as expected from Figure 1b $Ba(OH)_2$ based diode showed higher efficiencies for similar device architecture based on Cs_2CO_3, particularly in terms of maximum power efficiency increased by 1.5 times.

We also compared bipolar devices (with and without these interlayers) with hole-only devices (ITO/PEDOT:PSS/F8BT(~ 250 nm)/MoO_3/Au) and found that without interlayers, bipolar devices showed a similar current density to hole-only devices (holes injected from MoO_3/Au), as shown in **Figure 2**a. We also note that in the case of hole-only device there is no threshold voltage in contrast to the bipolar devices as shown in Figure 2a. As we discuss later, we consider the threshold arises when there is a barrier for hole extraction at the ZnO electrode, as depicted in Figure 2b (energy level values were measured by photoelectron spectroscopy, taken from our previous studies).[11,15] We get lower threshold voltage in the absence of $Ba(OH)_2$ and Cs_2CO_3 interlayers, and we consider that both interlayers have hole-blocking character. However, despite the different thickness of F8BT used in HyLEDs of Figure 1b and Figure 2a, we found threshold voltage were quite similar, i.e., ≈2 V. We also note that current density for holes is space-charge limited, which is consistent with our previous report.[7] However, devices with a $Ba(OH)_2$ interlayer showed a current density ten times lower, and the devices with Cs_2CO_3 interlayer were a further four times lower (see Figure 2a); such a reduced bipolar current density was also observed in blue emitting polyfluorene based HyLEDs with Cs_2CO_3,[21] which can be attributed to extraction barrier for dominant carriers, i.e., holes in these HyLEDs.

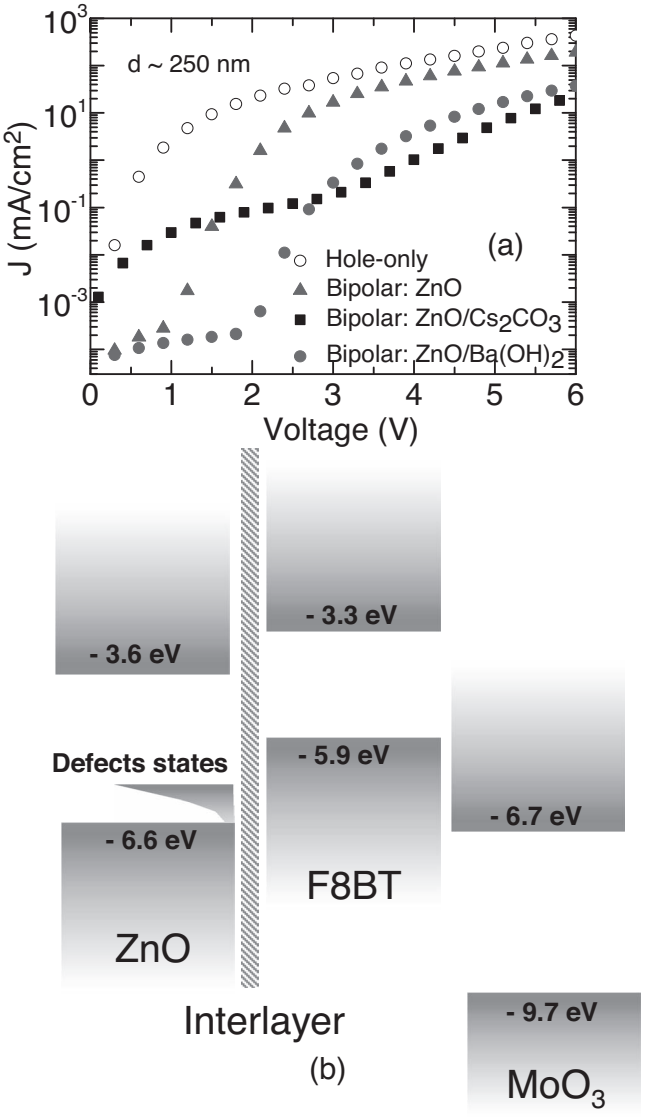

Figure 2. *J-V* characteristics of a) hole-only device (○) ITO/PEDOT:PSS/F8BT/MoO3/Au (current was injected from MoO3/Au side) bipolar device with Cs2CO3 interlayer (■), Ba(OH)2 interlayer (●), and without interlayer (solid Δ) in ITO/ZnO/Cs2CO3or Ba(OH)2/F8BT/Ca/Al structure. b) Schematic of energy level diagrams for various layers in HyLED.[10,11]

We have established that hole injection is not altered in these HyLEDs. We have measured many single-carrier electron-only devices (ITO/ZnO/interlayer/F8BT/Ca/Al) and find that $Ba(OH)_2$ is slightly better than Ca/Al top contact (see Supporting Information Figure S3). However, we find significant scatter in behaviour for these devices, and suspect that large electron current densities may be due to shunt leakage through diffusion of Cs^+ ions through the polymer layer.[7] We note that ZnO/$Ba(OH)_2$ was a better electron injector than Ca/Al in F8BT film in all batch of electron-only devices.

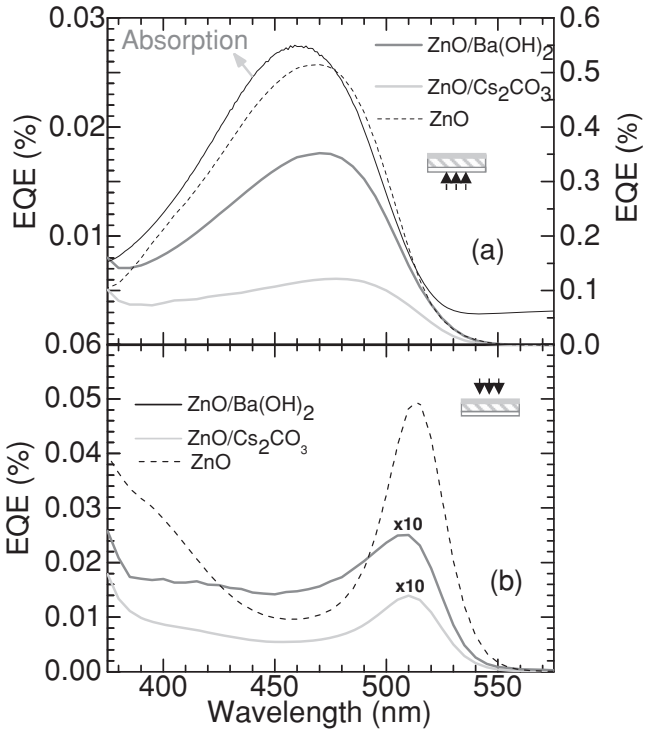

Figure 3. EQE as a function of illumination wavelength for HyLEDs based on Cs_2CO_3 (light grey) and $Ba(OH)_2$ (dark grey) and without interlayer (dash black), while illuminating from a) ITO electrode side along with UV-vis absorption spectrum of F8BT film on quartz substrate and b) MoO_3/Au side. F8BT film thickness is ≈250 nm.

A cyclical voltage sweep for HyLEDs was also carried out to show evidence for interfacial ionic charges.[22] $Ba(OH)_2$ interlayer based HyLEDs showed a clear hysteresis loop (see Supporting Information Figure S4a) for particular time interval of 100 ms between consecutive voltage steps of 0.1 V. In the case of Cs_2CO_3, overall current density is however reduced, the current on-set is at a higher bias as compare to the J–V curve of $Ba(OH)_2$ and no prominent hysteresis was observed (see Supporting Information Figure S4b).

2.3. Photovoltaic Measurements on HyLEDs

Photovoltaic measurements were carried out on the HyLEDs. We compared three kinds of device structures, namely ITO/ZnO/F8BT/MoO_3/Au; ITO/ZnO/Cs_2CO_3/F8BT/MoO_3/Au, and ITO/ZnO/$Ba(OH)_2$/F8BT/MoO_3/Au, keeping a F8BT film thickness of ≈250 nm. We performed spectral photocurrent measurements, illuminating HyLEDs from both the ITO side and the semi-transparent metal electrode (Au 20 nm) side, as shown in **Figure 3**. When illuminating from the ITO side, the photocurrent follows the F8BT absorption spectrum and shows a maximum charge generation at the absorption peak wavelength, i.e., ≈470 nm. However, while illuminating from the MoO_3/Au electrode the photocurrent spectral response peaks at edge of the absorption spectrum.[23] This measurement reveals that charge generation in this single layer diode is at the ZnO/F8BT interface. F8BT excitons are dissociated at ZnO/F8BT interface with electrons transferring to the ZnO and holes transported through the F8BT film towards the MoO_3/Au anode. The low EQE value observed in this system is primarily due to the requirement of light to be absorbed close to this interface and also due to possible formation of strongly bound charge-transfer state at ZnO/polymer interface.[24] Figure 3 shows that in the presence of interlayers the EQE drops down more than an order of magnitude.

We also carried out open-circuit voltage (V_{oc}) and short-circuit photocurrent (J_{ph}) measurements with respect to white-light intensity, using an AM1.5 solar simulator with different neutral-density optical filters. Intensity dependent V_{oc} studies (see Supporting Information Figure S5) suggest that there is significant back-recombination in absence of interlayers, where holes recombine with transferred electrons in ZnO. Therefore, V_{oc} was minimum (≈1 V) without the interlayer, maximum for $Ba(OH)_2$ interlayer and intermediate for $Cs_2(CO)_3$ (see Supporting Information Figure S5). In the cases of $Ba(OH)_2$ and Cs_2CO_3 based HyLEDs, we observed that $Ba(OH)_2$ based diodes gives higher V_{oc} than those using Cs_2CO_3 interlayers due to reduced dark current. In the case of intensity dependence of short-circuit photocurrent, (see Supporting Information Figure S5b) J_{ph} was found to be linear with respect to light intensity and consistent with spectral EQE measurements, i.e., highest photocurrent is for structures without interlayers due to relatively efficient charge separation at the ZnO/F8BT interface, and it is most poor in the case of Cs_2CO_3 based HyLEDs, due to diminished hole transport by diffusion of Cs^+ ions in F8BT.

2.4. Transient Photovoltaic (TPV) Studies

TPV studies were carried out on HyLEDs with and without inorganic interlayers, in order to obtain a photophysical insight of these interfaces and to understand further the steady-state measurements of these structures. TPV characteristics are shown in **Figure 4** and summarized in **Table 3**. TPV studies (using an inorganic blue LED source, λ_{em} = 470 nm, pulse width = 500 μs) indicated that in the absence of an interlayer there is a significant recombination loss of photogenerated carriers at the photoactive ZnO/F8BT interface. This results in a faster decay rate (τ = 34 μs, fitted by monoexponential decay) of the normalized TPV signal, and much lower V_{oc}. However, by introduction of interlayers we obtained significantly higher V_{oc} due to reduced recombination losses and, in particular, this is most evident in the case of the $Ba(OH)_2$ interlayer, which provides the highest V_{oc} (see Supporting Information Figure S6). These measurements were found to be in agreement with our steady state intensity dependent studies (see Supporting Information Figure S5).

2.5. Out-Coupling of Photons

Out-coupling is one of the major loss mechanisms in organic light emitting diodes, allowing only ≈20% of generated photons

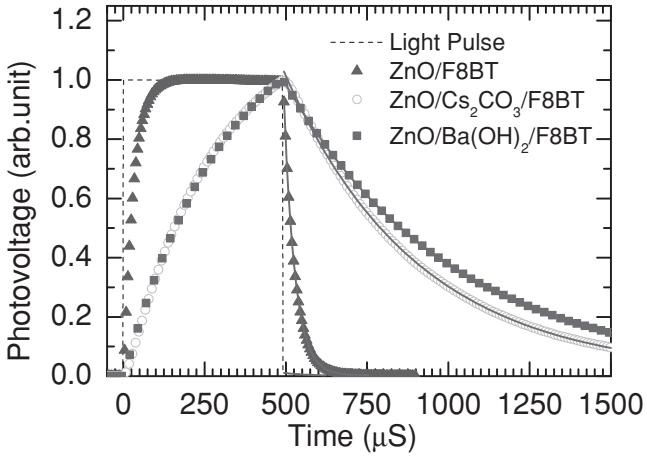

Figure 4. TPV measurements on ITO/ZnO/F8BT/MoO_3/Au (triangles); ITO/ZnO/Cs_2CO_3/F8BT/MoO_3/Au (circles); and ITO/ZnO/$Ba(OH)_2$/F8BT/MoO_3/Au (squares) using a light pulse of 500 μs duration. The light pulse is indicated with a dashed line. The decay of TPV signal after the light pulse is fitted using a single exponential equation.

to be out-coupled from the substrate surface.[25] We can reduce total internal reflection at the substrate/air interface by using an index-matched glass hemisphere with an index-matching oil onto the glass substrate (Supporting Information Figure S7),[26] and thus achieve even higher efficiency value upto 47 cd/A (see in Table 2). Further optimization of such out-coupling arrangements will in the future allow even higher values of luminance and efficiency to be achieved (also discussed in the Supporting Information).

3. Discussion

A luminance efficiency of ≈28 cd/A (EQE ≈ 9%) with power efficiency ≈9.0 lm/W was achieved in $Ba(OH)_2$ interlayer based HyLEDs. The higher EQE as compared to Cs_2CO_3 based HyLEDs (EQE 7.3%; power efficiency ≈ 6 lm/W) can be explained by higher η_{PL} (EQE α η_{PL}) value obtained for $Ba(OH)_2$ case, as showed in Table 1. The higher power efficiency in $Ba(OH)_2$ as compared to Cs_2CO_3 based HyLEDs can be explained by the nature of alkali vs alkaline metals based interlayer. Recent study on Cs_2CO_3 based HyLEDs revealed that diffusion of Cs_2CO_3 diminish hole transport in another polyfluorene polymer,[21] which can be a possible cause of reduced bipolar current, as compared to barium precursor based HyLEDs. As doubly-charged barium (Ba^{2+}) is known to have relatively poor diffusive properties into polymer films,[27] hence, in addition to providing a strong blocking interfacial effect, barium based interlayers do not affect bulk hole transport in F8BT.

We note that EQE (EQE = $\eta_{PL}\gamma_c\eta_s\eta_{out}$; where η_{PL} is PL quantum yield, γ_c is the charge carrier balance, η_s is the singlet formation ratio, i.e., 25%, and η_{out} is the out-coupling efficiency for the device structure) of $Ba(OH)_2$ based HyLEDs is higher than predicted by spin-statistics of organic semiconductors. The singlet exciton formation ratio with respect to triplet excitons on electrical injection was investigated recently in this HyLED architecture and the results suggested that triplet excitons contribute the formation of singlet states via a triplet-triplet annihilation (TTA) process and this ratio can reach up to 40% in steady-state condition by charge carrier recombination.[28] However, the present EQE values cannot be explained by TTA contribution only and there might be improved out-coupling in polymeric semiconductor based LEDs[29] and/or singlet exciton formation cross-section may be higher than triplet exciton formation in conjugated polymers.[30] Further study of the singlet versus triplet formation ratio is beyond the scope of this work and we limit ourselves to interfacial studies in this manuscript.

Photovoltaic studies revealed the influence of interlayers on photoinduced charge generation, which can be explained by derived excitons diffusion length (≈8 nm) and non-radiative quenching in the presence of interlayers from our optical studies. Interlayers act as an extra optical spacer between F8BT and ZnO, which results in further reduction in EQE. Photovoltaic measurements were also found to be consistent with the results obtained for LEDs characteristics, where in the absence of interlayers we found significant holes leakage current and $Ba(OH)_2$ provides better hole blocking character then leaky Cs_2CO_3 interlayer. These inorganic interlayers showed the reduced back-recombination and results in higher V_{oc}. TPV measurements further confirmed reduced recombination losses in terms of longer single exponential decay times for V_{oc} upon pulsed light illumination (see Figure 4 and Table 3) in the presence of interlayers.

Table 3. Transient photovoltage decay characteristics for HyLEDs with and without interlayers.

Structure	τ [μS]
ZnO/F8BT	34
ZnO/Cs_2CO_3/F8BT	405
ZnO/$Ba(OH)_2$F8BT	517

4. Conclusions

To summarize, we have investigated HyLEDs using solution processible Cs_2CO_3 and $Ba(OH)_2$ interlayers and found that the device efficiency with $Ba(OH)_2$ is significantly improved, which can be explained by reduced exciton quenching at cathode interface. The power efficiency is also ≈1.5 times higher for the $Ba(OH)_2$ interlayer (at 9 lm/W) as compared to the more commonly used Cs_2CO_3 interlayer. We attribute this improved device performance to the fact that Ba^{2+} with higher charge is less readily diffuse into the polymer bulk and does not affect bulk hole transport in F8BT. Hence, electron ejection is facilitated by the electric fields induced by accumulation of holes at the cathode, where $Ba(OH)_2$ outperform leaky Cs_2CO_3. Together with reduced exciton quenching at the interface, this results in lower operating voltages and hence, improved device efficiency and stability. Photovoltaic studies further confirm the role of

these interlayers as hole-blocking layers in agreement with LED studies. The use of a hemisphere for the enhancement of the outcoupling leads to a further improvement of device performance, the current efficiency reaches ≈47 cd/A corresponding to a 15% EQE and a power efficiency of 15 lm/W, with further room for improvement by optimization of the out-coupling structure.

5. Experimental Section

ITO substrates were cleaned sequentially in acetone and isopropanol in an ultrasonic bath for 10 min each, and were then heated to 400 °C in order to deposit zinc oxide by spray pyrolysis from the organic precursor zinc acetate dihydrate dissolved in methanol (80 mg/mL). $Ba(acac)_2$, $Ba(OH)_2$, and Cs_2CO_3 were dissolved in 2-methoxyethanol (7 mg/ml) (Fluka) at 80 °C and spin-coated onto the ZnO layer at 3000 rpm. $Ba(acac)_2$ was difficult to dissolve in most of the solvents, which might be related to its high hygroscopic nature. So most of the studies focused on $Ba(OH)_2$ based interlayers in the case of barium based interlayer. F8BT was dissolved in p-xylenes at 80 °C and spin-coated directly on top of the $Ba(OH)_2$ layer. Samples were then annealed at 155 °C under nitrogen for 1 hour. F8BT film thicknesses were varied by changing concentration from 3 mg/ml to 45 mg/ml for different samples. Finally, the samples were transferred to a thermal evaporation chamber (high vacuum of 1×10^{-6} mbar) for the deposition of MoO_3 (10 nm) (powder, 99.999% from Testbourne) and Au (70 nm) for light emitting diodes, or semitransparent Au (20 nm) for photovoltaic measurements. The devices were then encapsulated.

Electrcal and Optical Measurements: Current density (Keithley 2400 source measurement unit) and brightness (Keithley 2000 multimeter) versus applied voltage (Keithley 2400 sourcemeter) characteristics for the LEDs were measured in air using a calibrated reference Si photodetector. Photoluminescence decay kinetics was measured by time-correlated single photon counting (TCSPC), using a polymer film thickness of 15 nm. The excitation source was a pulsed $\lambda_{excitation}$ = 470 nm, 80 ps full width at half maximum, 10 MHz diode laser (PicoQuant LDH400) and the luminescence was detected using a microchannel plate photomultiplier (Hamamatsu Photonics) coupled to a monochromator and TCSPC electronics (Lifespec-ps and VTC900 PC card, Edinburgh Instruments). With the same 470 nm laser excitation source, photoluminescence spectra were taken using a 500 mm spectrograph (SpectraPro2500i, Princeton Instruments) combined with a CCD camera (Acton 100-F, Princeton Instruments).

Photovoltaic Measurements: Devices for photovoltaic measurements were prepared in similar fashion to HyLEDs, however, the F8BT thickness was reduced to 250 nm and the top Au electrode thickness was 20 nm (conducting semitransparent electrode) to allow illumination from the anode side.

For EQE measurements, a 100 W halogen lamp and a Bentham monochromator were used. The measurements were performed as a function of wavelength at intensities of ≈1 mW/cm^2. To measure the *I–V* curve, V_{oc} and J_{sc} of the device under AM1.5 conditions, an Oriel 81160-1000 solar cell simulator was used and the intensity of light was varied by using neutral density filters.

Transient Photovoltaic Studies: For the TPV measurement a high-brightness $\lambda_{emission}$ = 470 nm blue LED (Kingbright, L-7104VGC-H) was used as the light source and a Hewlett Packard (HP) 8116A pulse/function generator was used as the power supply for the LED. An Agilent DSO6052A digitizing oscilloscope with input impedance of 1 MΩ was used to measure the transient photovoltage pulse. To calibrate the system a commercial photodetector (BPX-65 silicon solar cell) and LEDs were used and results for transient PV with respect to the applied light pulse were presented.

Optical Out-Coupling Setup: A 8 mm diameter hemisphere was mounted on top of glass substrate of dimensions 12 mm × 12 mm × 1.2 mm, with an interlayer of index-match oil. This substrate contained 8 HyLED pixels with a size of 1.5 mm × 3 mm, which placed restrictions on the optimization of out-coupling using this setup, as discussed in the Supporting Information. To check the influence of the hemisphere on emission patterns, an angular stage coupled with a multimode optical fiber was used. EL emission was collected using an optical fiber coupled USB-4000 ocean optics spectrometer at different angles from 0° to 85°. Emission patterns were taken into account when calculating the enhancement in out-coupled EL emission.

Supporting Information

Supporting Information is available from the Wiley Online Library or from the author.

Acknowledgements

The authors thank Dr. Chris Finlayson of Aberystwyth University (UK) for helpful discussions. The authors acknowledge the EPSRC for support and Cambridge Display Technology Ltd, UK for funding and materials.

Received: March 27, 2012
Published online: June 8, 2012

[1] J. H. Burroughes, D. D. C. Bradley, A. R. Brown, R. N. Marks, K. Mackay, R.H. Friend, P.L. Burns, A.B. Holmes, *Nature* **1990**, *347*, 539.
[2] a) K. Morii, M. Ishida, T. Takashima, T. Shimoda, Q. Wang, M. K. Nazeeruddin, M. Gratzel, *Appl. Phys. Lett.* **2006**, *89*, 223511; b) P. D. Bruyn, D. J. D. Moet, P. W. M. Blom, *Org. Elec.* **2012**, *13*, 1023.
[3] H. J. Bolink, E. Coronado, D. Repetto, M. Sessolo, *Appl. Phys. Lett.* **2007**, *91*, 223501.
[4] H. J. Bolink, E. Coronado, D. Repetto, M. Sessolo, E. M. Barea, J. Bisquert, G.-B. Germa, J. Prochazka, L. Kavan, *Adv. Funct. Mater.* **2008**, *18*, 145.
[5] D. Kabra, M. H. Song, B. Wenger, R. H. Friend, H. J. Snaith, *Adv. Mater.* **2008**, *20*, 3447.
[6] H. J. Bolink, E. Coronado, J. Orozco, M. Sessolo, *Adv. Mater.* **2009**, *21*, 79.
[7] D. Kabra, L. P. Lu, M. H. Song, H. J. Snaith, R. H. Friend, *Adv. Mater.* **2010**, *22*, 3194.
[8] T. Gershon, *Mater. Sci. Technol.* **2011**, *27*, 1357.
[9] M. Sessolo, H. J. Bolink, *Adv. Mater.* **2011**, *23*, 1829.
[10] M. Kröger, S. Hamwi, J. Meyer, T. Riedl, W. Kowalsky, A. Kahn, *Org. Electron.* **2009**, *10*, 932.
[11] M. C. Gwinner, Y. Vaynzof, K. K. Banger, P. K. H. Ho, R. H. Friend, H. Sirringhaus, *Adv. Funct. Mater.* **2010**, *20*, 3457.
[12] H. Choi, J. S. Park, E. Jeong, G.-H. Kim, B. R. Lee, S. O. Kim, M. H. Song, H. Y. Woo, J. Y. Kim, *Adv. Mater.* **2011**, *23*, 2759.
[13] J. Fang, B. H. Wallikewitz, F. Gao, G. Tu, C. Muller, G. Pace, R. H. Friend, W. T. S. Huck, *J. Am. Chem. Soc.* **2011**, *133*, 683.
[14] J. Huang, Z. Xu, Y. Yang, *Adv. Funct. Mater.* **2007**, *17*, 1966.
[15] Y. Vaynzof, D. Kabra, L. L. Chua, R. H. Friend, *Appl. Phys. Lett.* **2011**, *98*, 113306.
[16] A. Crispin, A. Jonsson, M. Fahlman, W. R. Salaneck, *J. Chem. Phys.* **2001**, *115*, 5252.
[17] M. Kuik, H. T. Nicolai, M. Lenes, G.-J. A. H. Wetzelaer, M. Lu, P. W. M. Blom, *Appl. Phys. Lett.* **2011**, *98*, 093301.
[18] G. A. H. Wetzelaer, M. Kuik, H. T. Nicolai, P. W. M. Blom, *Phys. Rev. B* **2011**, *83*, 165204.
[19] M. A. Stevens, C. Silva, D. M. Russell, R. H. Friend, *Phys. Rev. B* **2001**, *63*, 165213.

[20] M. K. Fung, S. L. Lai, S. W. Tong, S. N. Bao, C. S. Lee, W. W. Wu, M. Inbasekaran, J. J. O'Briend, S. T. Lee, *J. Appl. Phys.* **2003**, *94*, 5763.
[21] L. P. Lu, D. Kabra, K. Johnson, R. H. Friend, *Adv. Funct. Mater.* **2012**, *22*, 144.
[22] W. Brutting, H. Riel, T. Beierlein, W. Riess, *J. Appl. Phys.* **2001**, *89*, 1704.
[23] M. G. Harrison, J. Gruner, G. C. W. Spencer, *Phys. Rev. B* **1997**, *55*, 7831.
[24] Y. Vaynzof, A. A. Bakulin, S. Gelinas, R. H. Friend, unpublished.
[25] Y. Sun, S. R. Forrest, *Nat. Photonics* **2008**, *2*, 483.
[26] S. Reineke, F. Lindner, G. Schwartz, N. Seidler, K. Walzer, B. Lussem, K. Leo, *Nature* **2009**, *459*, 234.
[27] F. Scheiba, N. Benker, U. Kunz, C. Roth, H. Fuess, *J. Power Sources* **2008**, *177*, 273.
[28] B. H. Walikewitz, D. Kabra, S. Gélinas, R. H. Friend, *Phys. Rev. B* **2012**, *85*, 045209.
[29] a) J.-S. Kim, P. K. H. Ho, N. C. Greenham, R. H. Friend, *J. Appl. Phys.* **2000**, *88*, 1073; b) J. Frischeisen, D. Yokoyama, A. Endo, C. Adachi, W. Brütting, *Org. Electron.* **2011**, *12*, 809.
[30] M. Wohlgenannt, K. Tandon, S. Mazumdar, S. Ramasesha, Z. V. Vardeny, *Nature* **2001**, *409*, 494.